

The Superconducting Super Collider

Received by OSNL
JUL 16 1990

A Progress Report on Fermilab Experiment E778 An Experimental Study of the SSC Magnet Aperture Criterion

A. Chao, D. Johnson, S. Peggs, J. Peterson, and L. Schachinger
SSC Central Design Group

R. Meller, R. Siemann and R. Talman
Cornell University

L. Vos
CERN

P. Morton
Stanford Linear Accelerator Center

and
D. Edwards, D. Finley, R. Gerig, N. Gelfand,
M. Harrison, R. Johnson, N. Merminga, and M. Syphers
Fermi National Accelerator Laboratory

January 12, 1988

DISTRIBUTION OF THIS DOCUMENT IS UNLIMITED

*DO NOT MICROFILM
COVER*

DISCLAIMER

This report was prepared as an account of work sponsored by an agency of the United States Government. Neither the United States Government nor any agency thereof, nor any of their employees, makes any warranty, express or implied, or assumes any legal liability or responsibility for the accuracy, completeness, or usefulness of any information, apparatus, product, or process disclosed, or represents that its use would not infringe privately owned rights. Reference herein to any specific commercial product, process, or service by trade name, trademark, manufacturer, or otherwise does not necessarily constitute or imply its endorsement, recommendation, or favoring by the United States Government or any agency thereof. The views and opinions of authors expressed herein do not necessarily state or reflect those of the United States Government or any agency thereof.

DISCLAIMER

Portions of this document may be illegible in electronic image products. Images are produced from the best available original document.

SSC--156

DE90 013788

A Progress Report on Fermilab Experiment E778

AN EXPERIMENTAL STUDY OF THE SSC MAGNET APERTURE CRITERION

A. Chao, D. Johnson, S. Peggs, J. Peterson, and L. Schachinger
SSC Central Design Group*
c/o Lawrence Berkeley Laboratory, Berkeley, CA 94720 U.S.A.

R. Meller, R. Siemann, and R. Talman
Newman Laboratory of Nuclear Studies, Cornell University,
Ithaca, NY 14853 U.S.A.

L. Vos
SPS Division, CERN, 1211 Geneva 23, Switzerland

P. Morton
Stanford Linear Accelerator Center, Stanford, CA 94305 U.S.A.

and

D. Edwards, D. Finley, R. Gerig, N. Gelfand, M. Harrison, R. Johnson, N. Merminga,
and M. Syphers
Fermi National Accelerator Laboratory, Batavia, IL 60510 U.S.A.

January 12, 1988

*Operated by Universities Research Association for the U. S. Department of Energy

Progress Report on E778

AN EXPERIMENTAL STUDY OF THE SSC MAGNET APERTURE CRITERION

Introduction

The magnetic field quality specification used in the SSC Conceptual Design Report is based on the imposition of bounds to the departure from linear behavior in the oscillation of single particles about their closed orbits. The specification is physically reasonable, but it is important to give serious attention to the values assigned to the parameters in the criterion. This experiment (E778) is part of that effort.

If the betatron oscillations of a particle in a synchrotron are linear, then the oscillation amplitude will be a constant of the motion. If there is no coupling between the two transverse degrees of freedom, the projections of the amplitude on the horizontal and vertical planes will each be an invariant. A turn-by-turn plot of the vertical projection versus the horizontal projection will yield a single point.

Nonlinearities in the magnetic fields will lead to gradual (on the time scale of a betatron oscillation period) changes in the magnitudes of the transverse amplitude projections. The single point of the turn-by-turn plot will develop, in general, into an area. The distance of a point within this area to the mean position of all the points is a measure of the change of amplitude. The criterion places a limit on the ratio of this change to the mean amplitude. In particular, the rms value of this fractional excursion, termed the "smear," is to be less than 7% within the aperture used for routine beam operations.

The principal aims of experiment E778 are to determine if the smear is predictable from calculation, if the 7% bound is appropriate, and if modification of the criterion is necessary. The Tevatron was considered a suitable laboratory for this activity because it is a proton accelerator with excellent linear behavior; moreover there was a substantial number of sextupole magnets already installed that could be used as controllable sources of nonlinearity.

This progress report is a summary of the effort on this experiment to date and preliminary analysis of the data. During the collider run last winter, six shifts were used to commission the equipment and develop techniques. The bulk of the data on which this analysis is based were taken during ten shifts in mid-May, just after collider operation was terminated.

Background for the Experiments

Phase Space Measurements

The beam position monitors in the Tevatron are capable of recording the motion of the center of charge of the beam for one thousand consecutive turns. The positions at two neighboring monitors, coupled with a knowledge of the intervening optics, can be used to find the transverse velocity of the beam at either monitor. Thus, a phase space plot can be obtained for the turn-by-turn motion.

Figures 1a and 1c show turn-by-turn plots in the Tevatron as recorded by two neighboring position monitors in the horizontal plane. A coherent betatron oscillation was induced in the circulating beam by firing a kicker magnet fifty turns after the beginning of the plot. That the decrease in amplitude is modest over the thousand turns is an indication of near-linear behavior. Figures 1b and 1d display the Fourier transforms of the two position signals, and give the fractional part of the betatron oscillation tune.

In Figure 2, similar data is displayed in normalized phase space coordinates; the horizontal axis is position and the vertical is the appropriate conjugate variable so that the plot is the familiar circle of simple harmonic motion. If the position variable is x and the angle with respect to the unperturbed orbit is x' , then in terms of the conventional Courant-Snyder parameters, this conjugate variable is $\beta x' + \alpha x$.

In 1985, when this procedure for displaying phase space motion became routinely available in the control room at Fermilab, some initial studies were made of the perturbation of the motion by nonlinearities. In particular, eight sextupoles were used to excite the resonance at the betatron oscillation tune of $19 \frac{1}{3}$. Figure 3 shows a case in which the small amplitude tune was 19.34. A kicker produced an initial amplitude so that a particle at the centroid would perform stable motion close to the separatrix. As expected, the circle is deformed into the triangle characteristic of this resonance.

A natural extension of this technique employs four position monitors - two in each transverse degree of freedom - to obtain four dimensional phase space information. Though some preliminary data have been recorded in this mode, the studies to date have concentrated on one degree of freedom and the problems of representing four dimensional phase space will not be pursued here.

Sextupoles Used in E778

For this experiment, 16 additional sextupoles were commissioned. The superconducting magnets themselves had been installed when the Tevatron was constructed, but cables, power supplies, and controls still needed to be supplied. Including the 8 elements used in the earlier studies, the resulting sextupole complement is 16 normal sextupoles at stations 22, 24, 26, 28, 32, 34, 36, 38 in C and F sectors and 8 skew sextupoles at stations 12, 14, 16, 18, 23, 27, 37, 43 in D sector. The skew sextupoles were not used in the studies reported here.

The normal sextupoles are powered in pairs by 8 supplies, so a variety of configurations is possible. For this run, it was elected to power them so as to produce a strong third-integer resonance driving term. Measurements were performed at tunes far from the $1/3$ resonance to study the more complicated phase space structure exhibited there than that examined in the earlier work. Figure 4 and Figure 5 contrast the expected near-resonance and far-from-resonance behavior in the presence of only one sextupole as obtained from a tracking program. When the tune is near resonance - at 19.35, for example - the particle flow in phase space is along contours as exhibited in Figure 4. Far from resonance, at a tune of 19.42, the phase space contours become those in Figure 5.

The striking feature of Figure 5 is the appearance of resonance "islands." Since the unperturbed betatron tune is 19.42 in this figure, the particle tune varies from 19.42 at the origin to 19.333 at the separatrix. (Technically, the separatrix only exists when the discrete sextupoles are replaced by a smooth approximation.) At an intermediate amplitude, the sextupole generates the five islands characteristic of a fifth-order resonance. The phase space of Figure 4 also contains islands, but their orders are so large that they are difficult to see on the scale of the figure.

Measurements as Planned

The studies were organized in three experiments. All three were carried out at the Tevatron injection energy of 150 GeV. Necessary preliminaries included verification that the normalized emittance (95%) of the injected beam was at or below 15π mm-mrad, orbit adjustment at the nonlinearities to minimize tune shifts and other off-center effects, reduction of horizontal-vertical coupling by skew quadrupoles and tune split, reduction of chromaticity to 3 units or less, and minimization of coherent synchrotron oscillations at injection.

The first experiment consisted of a comparison between predicted and measured smear at four sextupole excitations from zero to full strength. After injection, the sextupoles were ramped up to the

desired setting in 10 seconds, then, after a further 10 second delay, a coherent betatron oscillation was induced by firing the Tevatron injection kicker. At each of several values of the horizontal tune, three kick amplitudes were employed, bounded from above by the onset of beam loss in the bare Tevatron. The principal data recorded at each condition were the turn-by-turn signals from two monitors, and the beam intensity through the supercycle.

In order to indicate the expected magnitudes, Figure 6 shows a calculation of the smear versus initial oscillation amplitude for the various sextupole excitations at a horizontal tune of 19.42. The calculation for Figure 6 is based on a single particle. Some idea of the effect of the finite emittance is suggested by Figure 7, which shows the calculated initial particle distribution of the kicked beam and the separatrix for two different kick amplitudes. An emittance of 15π mm-mrad was used for this figure.

The second experiment was an attempt to correlate the sextupole excitation with a performance degradation, either in the injected beam behavior or in the dynamic aperture. In the first case, the object was to look for greater difficulty in maintaining reliable low energy operation at higher sextupole strength. As the sextupole excitations are increased the dynamic aperture will decrease until it is within the vacuum chamber. The limiting beam size can be measured with flying wires while blowing up the beam with the dampers, and the results compared with calculation.

The final experiment was to be a study of the effects of tune modulation on particle stability. This experiment was more exploratory in nature than the others above, and related to long term stability questions. The tune was to be modulated at a range of frequencies between 300 and 2500 Hz and the dynamic aperture measured as a function of sextupole excitation. At low frequencies, the onset of chaos is expected, leading to a reduction of dynamic aperture if the chaotic region extends out to large amplitudes.

Experimental Techniques and Data Reduction

Single Particle Considerations

If the beam were a single particle, then at first glance the calculation of the smear would reduce to a simple matter of minimizing an appropriate least squares sum. The variables used in the minimization represent lattice functions and closed orbit offsets at the beam position monitors, which thereby are determined from the data.

But even in the single particle model, a number of other factors must be taken into account. The finite resolution of the beam position monitors is itself a source of smear. The resolution of the

monitors in use in this experiment was improved to 80 microns (the normal resolution is 160 microns), and this contribution to the smear may be subtracted in quadrature from the result of the above minimization.

To compensate for linear coupling between the two transverse degrees of freedom, the skew quadrupoles were adjusted so that less than 10% of the amplitude of a horizontal oscillation coupled over into the vertical when the tunes were split by approximately 0.1. The closed orbit was adjusted at each sextupole location so that both the closed orbit distortion and the small amplitude tune shift caused by the sextupole excitation were adjudged to be negligible. Occasional changes in the chromaticity circuits were made to compensate for the time variation of the sextupole moment in the main bending magnets.

Multiparticle Considerations

The finite emittance and momentum spread of the real beam make for difficulties in both the experimental procedures and in the data analysis. In principle, the decoherence of the turn-by-turn signal that arises from chromaticity can be eliminated and indeed that is straightforward at zero excitation of the additional sextupoles. However, the additional sextupoles introduce non-negligible chromaticity on their own. For the data reduction to date, a calculation of this correction has been used pending direct measurement.

But the dominant source of decoherence is the nonlinear tune variation with amplitude caused by the sextupoles. Figure 8 illustrates the loss of coherent beam centroid motion at progressively higher sextupole excitations. The extraction of the phase space distortion in the face of this effect relies on a reconstruction of a single-particle motion by fitting a Gaussian to the apparent amplitude reduction. Such a fit is shown in Figure 9. By fitting over a variable number of turns, one can determine the smear and also its stability versus turn number. The result for one experimental condition is shown in Figure 10.

The several corrections and fitting procedures of this and the preceding subsection are incorporated in a program, Tevex, written specifically for this experiment. This is the principal program used in the reduction of the smear data.

Results

Phase Space Distortion and Smear

Measurements were made at sextupole excitations of 15, 30 and 50 amperes for horizontal tunes in steps of 0.01 from 19.37 to 19.42 with oscillations generated by kicker voltages of 5, 8, and 10 kV. In the bare Tevatron, the corresponding oscillation amplitudes are roughly 2, 3, and 4 mm. The vertical tune was set to 19.46. A limited number of measurements were recorded at zero sextupole excitation.

The smear of the bare Tevatron is characterized by Figure 11, confirming that in the absence of the additional sextupoles the smear is indeed small. The finite resolution of the beam position monitors contributes about 1% to the observed smear. For the bare Tevatron measurements, this contribution was subtracted in quadrature to yield the results shown. This correction is negligible for the data taken with sextupoles energized.

A typical set of experimental data and analysis by Tevex is displayed in Figure 12 for a sextupole excitation of 15 amperes and a kick amplitude of 5 kV. For the same set of parameters, simulation results from three tracking programs were analyzed by Tevex and the results are displayed in Figures 13 through 15. The agreement between experiment and simulation is excellent for this set.

The results of various kick amplitudes and tunes for a sextupole excitation of 15 amperes are summarized in Figure 16. The aperture criterion was stated in terms of the behavior of a single particle. In that spirit, the calculated curves in the figure relate to a single particle. A comparison between single particle and multiparticle simulations has been used to convert the observed smear of the beam to that of a single particle.

Problems arise at higher excitation. One need only contrast the correspondence between tracking and measurement as revealed in Figures 17 and 18 with their counterparts at 15 amperes. The smear does not increase as predicted. Even more puzzling, the decoherence predicted by tracking is faster than that which is observed. A dramatic reduction in emittance due to beam loss could increase the coherence time, as illustrated by Figure 19 where the simulation has employed a factor of four reduction in emittance. But no beam loss was observed for this set of data.

Injection Experiment and Dynamic Aperture

The injection experiment consisted of injecting onto the closed orbit and off of the closed orbit by 1.5 mm with the sextupoles on at excitations of 0, 15, 30, 40, 45, and 50 amperes and recording the following data:

- First turn position monitor data
- Closed orbit at injection
- Turn-by-turn data at injection
- Flying wire data at injection
- Flying wires 9 seconds after injection
- Beam intensity versus time

At each sextupole setting, the orbit was reclosed and the tune adjusted to the desired value. The experiment was performed at tunes of 19.38 and 19.42.

Even at the highest excitations, the first three items revealed no significant variation or deterioration in information content. For instance, closed orbits a few milliseconds after injection differ by less than a millimeter for sextupole excitations of 0 and 45 amperes. The conclusion is that it would be possible to diagnose and correct injection problems in the presence of these strong nonlinearities.

The unexpected results were in the long term losses. Figure 20 is a summary of the observations. The fractional beam loss in the first five seconds after injection is plotted versus sextupole current. In each case, there is apparently a threshold sextupole current above which loss is found. Much of the loss is slow, as shown in Figure 21.

The physics of the loss is not understood. The time structure of the early loss as seen on the scintillation counters associated with the flying wires contains a component at the synchrotron oscillation frequency, thus the longitudinal motion may play a role.

The dynamic aperture measurement was a straightforward matter of increasing the beam emittance by injecting noise into the dampers, and observing the resulting beam size limit with the flying wires. The relevant results are presented in Table 1. At 15 amperes, the calculated dynamic aperture is outside of the physical aperture; at the higher currents the experimental results are smaller than the prediction from short-term tracking of on-momentum particles.

Table 1

<u>Sextupole Current</u>	<u>Dynamic Aperture (full width, mm)</u>	
	<u>measured</u>	<u>calculated</u>
15 Amperes	13*	27
30 Amperes	10.5	13.5
50 Amperes	6.5	8

*physical aperture smaller
than dynamic aperture

Tune Modulation and Islands

Referring to Figure 5, it is conceivable that with a particular kick amplitude and orientation, some fraction of the beam could become trapped in resonance islands. The detection of such trapping turned out to be surprisingly easy, for in the presence of decoherence of the rest of the beam, the trapped particles continue to oscillate in a coherent fashion, as is demonstrated in Figure 22.

A spectrum analyzer verified that this coherent motion continued throughout the ten seconds before the sextupoles ramped down. Both the turn-by-turn data and the spectrum analyzer showed that the sustained signals were associated with tunes whose fractional parts were $2/5$, $3/7$, $5/13$ as would be expected. As expected, the persistent signal at, for instance, $2/5$ was no longer present if the fractional part of the small amplitude tune was reduced below $2/5$.

Tune modulation was found to influence the lifetime of the persistent tune lines associated with particles trapped in islands. A particular set of results is shown in Figure 23. The islands break up at the higher frequencies with the departure from adiabaticity.

Proposed Future Measurements

Comparison of Tracking and Measurement

The source of the transition between agreement at 15 ampere sextupole excitation and disagreement at 30 amperes needs to be identified. It is proposed to take data at additional current settings to define the range of agreement. Some improvements in experimental technique are possible. The chromaticity with the sextupoles on should be more closely controlled, and so radial displacement through frequency change will be used to measure this quantity. By scraping the beam, the effect on the decoherence and on the calculation of smear of varying the emittance will be extracted. It is likely that the effect of varying the intensity at constant emittance can be explored through the use of rf manipulations in the Main Ring synchrotron.

Injection and Dynamic Aperture

In the injection experiment, the outstanding puzzle is the long term beam loss. It is desired to compare the loss in a typical condition with rf on and off, and to repeat the measurement as a function of beam intensity. It would be useful to repeat the dynamic aperture measurement and include the influence of closed orbit distortions.

Resonance Islands

A major upgrade of the turn-by-turn hardware and software is in progress in preparation for the next opportunity to take data on this phase of the experiment. When the Tevatron beam position monitor system was designed, one thousand turns and eight-bit accuracy was well suited to the intended purposes. For the study of the low level, persistent signals associated with resonance islands, an improvement in the resolution is needed.

The system will be extended to the 100,000 turn level with 12 bit resolution. The intensity on each turn will also be recorded to permit a detailed reconstruction of beam loss patterns. For the purposes of this experiment, readout will be to a dedicated computer running the analysis software. If this upgrade is determined to be useful for other purposes at Fermilab, a more permanent arrangement will be found. It is interesting to note that, when applied to the Main Ring, the turn-by-turn data could cover a complete beam cycle.

The turn-by-turn upgrade should confirm beyond any doubt that the long term tune lines observed earlier this year arise from trapping in islands. Of more interest, it is proposed to make the first direct measurement of island widths and to compare the results with theoretical predictions. For a particular set of conditions, one can predict the amplitude, orientation, and size of a chain of resonance islands, such as the one shown in Figure 5. Therefore the number of particles trapped may be predicted for a specific kick amplitude. This number may also be obtained experimentally from the beam position monitor signal, and so prediction and measurement can be compared in this intriguing aspect of phase space structure.

During the last run, very little time was devoted to tune modulation. With reference to Figure 24, the three points shown correspond to those studied last May. This figure may be broken into several regimes, although the dividing lines have not been established experimentally. To the right of the vertical line the particle motion is stable; the diagonal dividing line is the rough boundary between no sidebands and multiple sidebands due to frequency modulation. To the left of the vertical line, the sidebands overlap, leading to the potential of chaotic behavior. But this side of the figure is divided also into two areas; at sufficiently low frequency, a particle will remain trapped within the "moving" island, and it is plausible to locate the diagonal line so that the three experimental points are within this region.

It is proposed to perform sufficient measurements to identify the several regions. With the existing system, modulation amplitudes of 0.01 and modulation tunes of 0.01 are achievable following minor hardware modification to the existing slow-spill feedback systems.

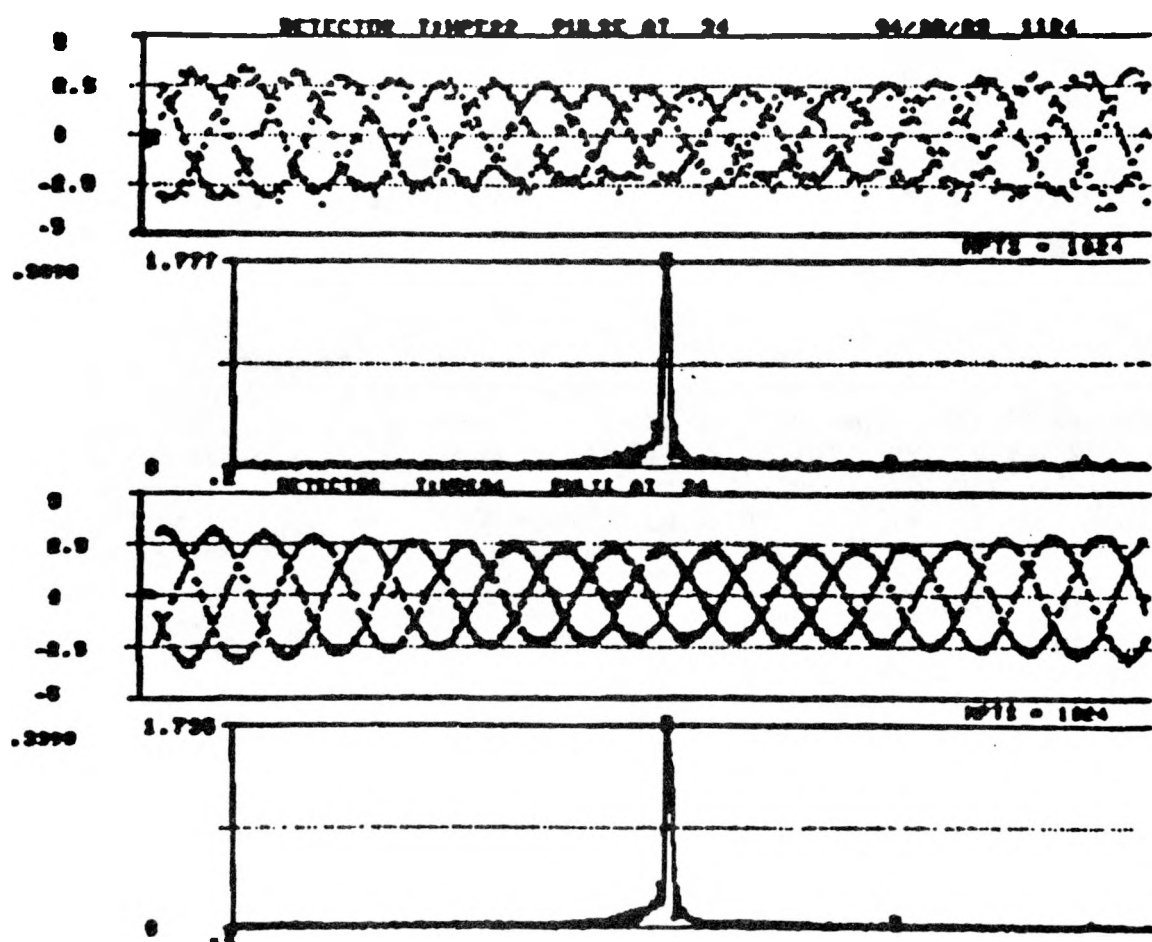


Fig. 1. (a) and (c) are the output of two neighboring beam position monitors for 1024 turns. A coherent betatron oscillation was initiated by firing kicker magnet some 50 turns after the beginning of the trace. The fourier transforms are shown in (b) and (d); the fractional part of the tune is 0.34.

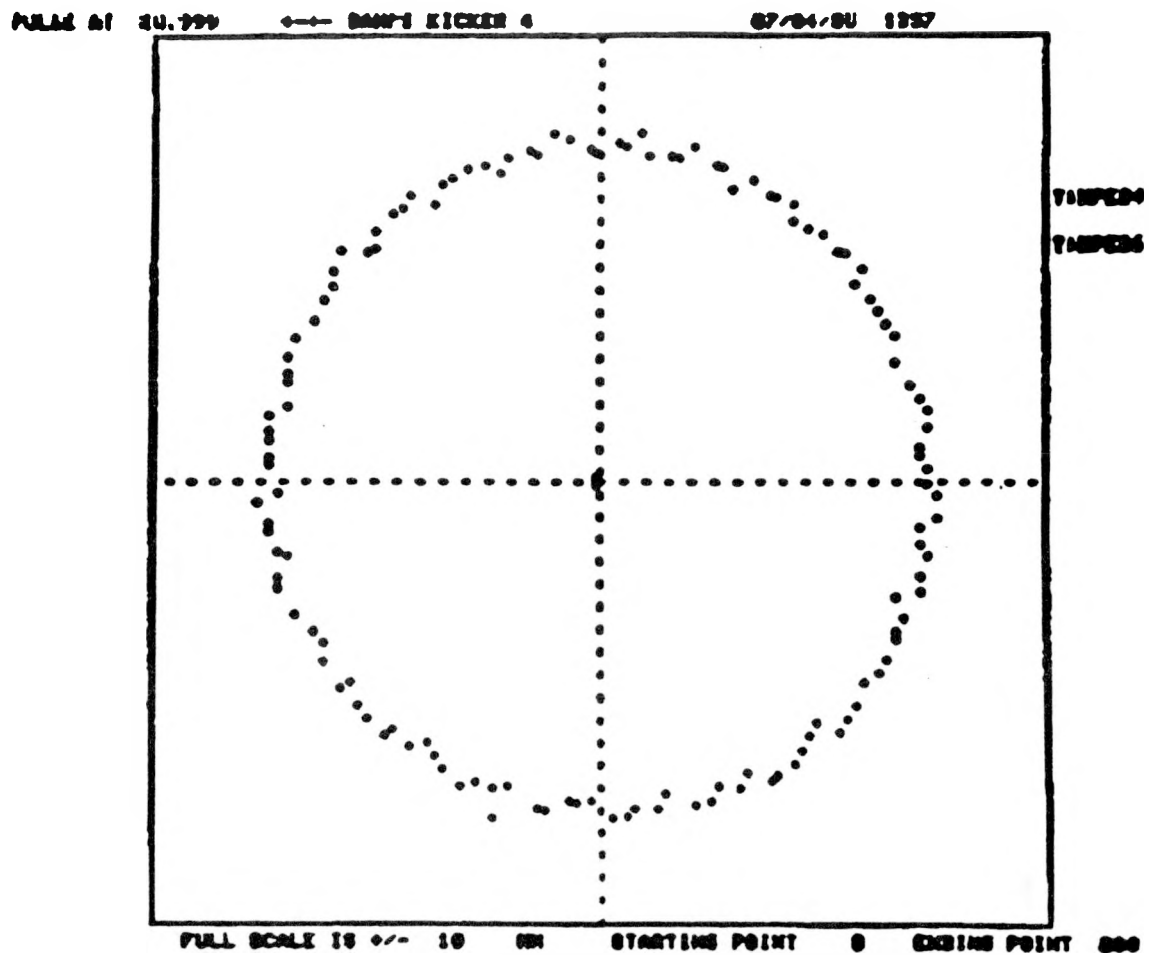


Fig. 2. Phase space plot constructed from data similar to that shown in Fig. 1. The horizontal axis is displacement, x , from the central orbit in mm. In order to obtain the characteristic circle of simple harmonic motion, the vertical axis is chosen to be $\beta x' + \alpha x$, where x' is the slope of the trajectory.

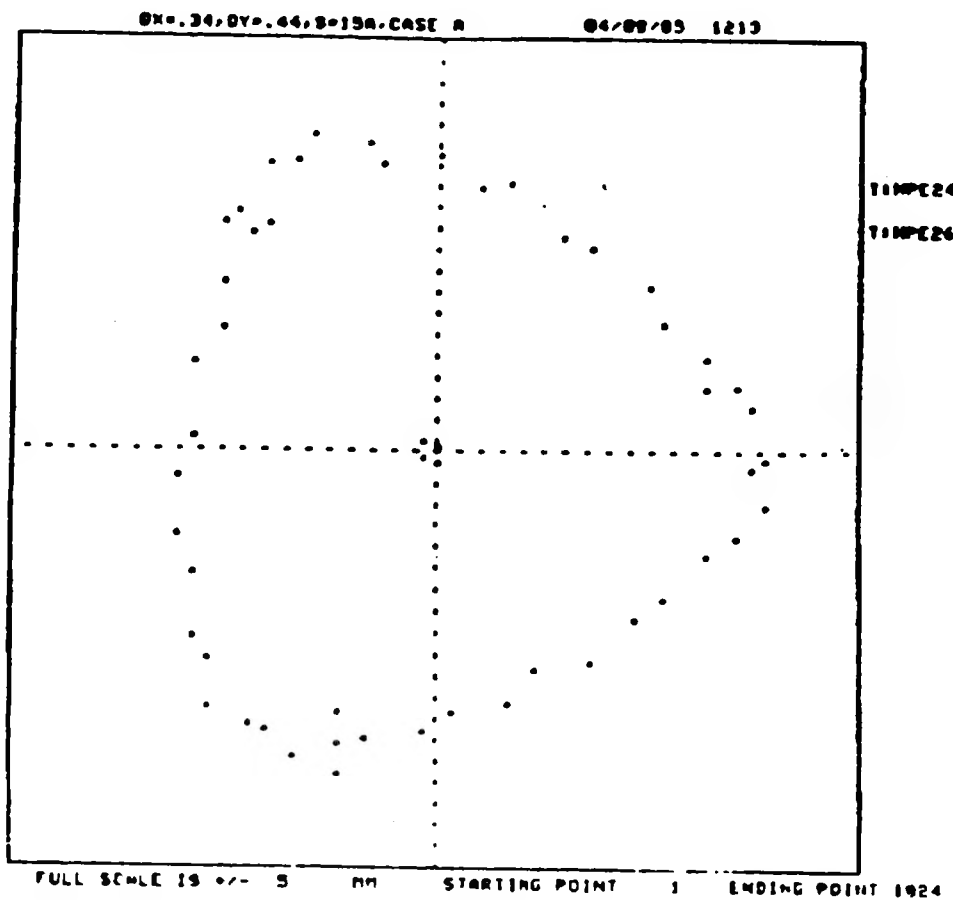


Fig. 3. Phase space plot from experimental data for betatron oscillation of amplitude close to third-integer resonance separatrix.

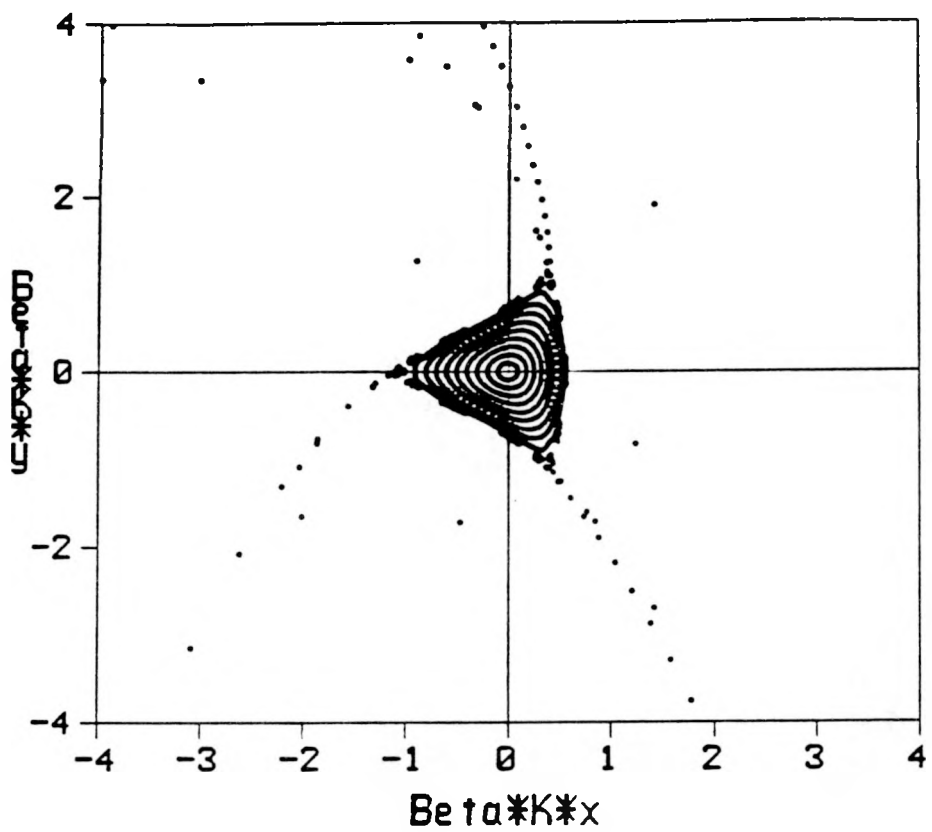


Fig. 4. Simulation of phase space for fractional part of the tune close to $1/3$ in the presence of a single sextupole.

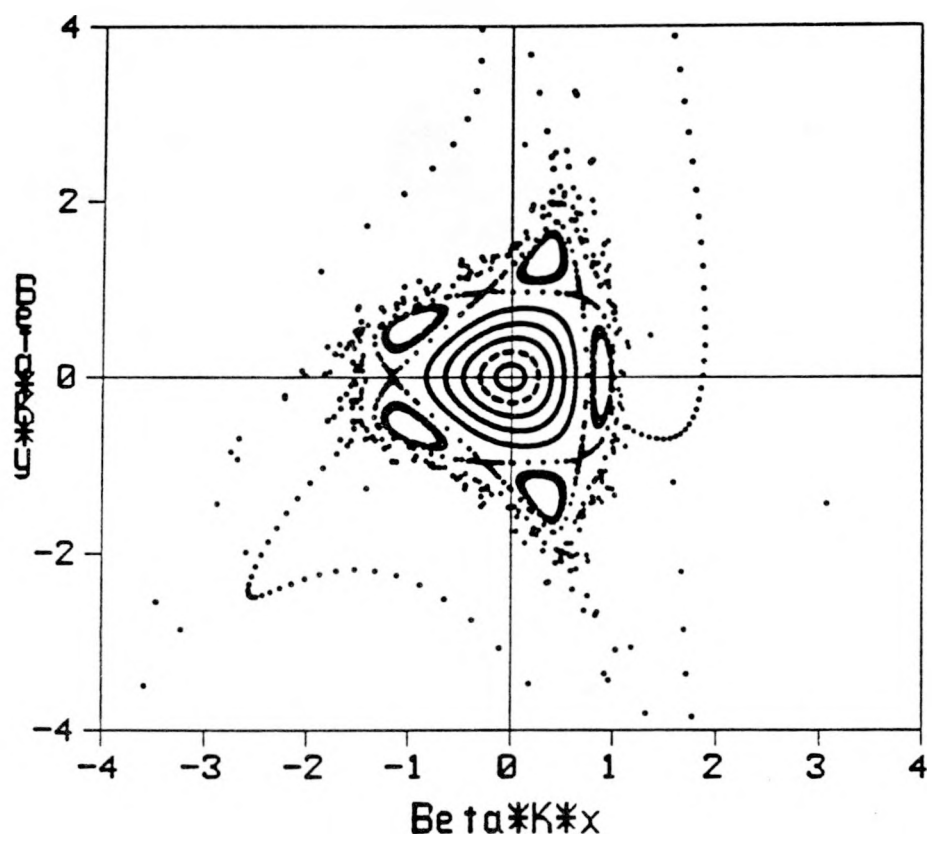


Fig. 5. Simulation of phase space for fractional part of the tune at 0.42 in the presence of a single sextupole.

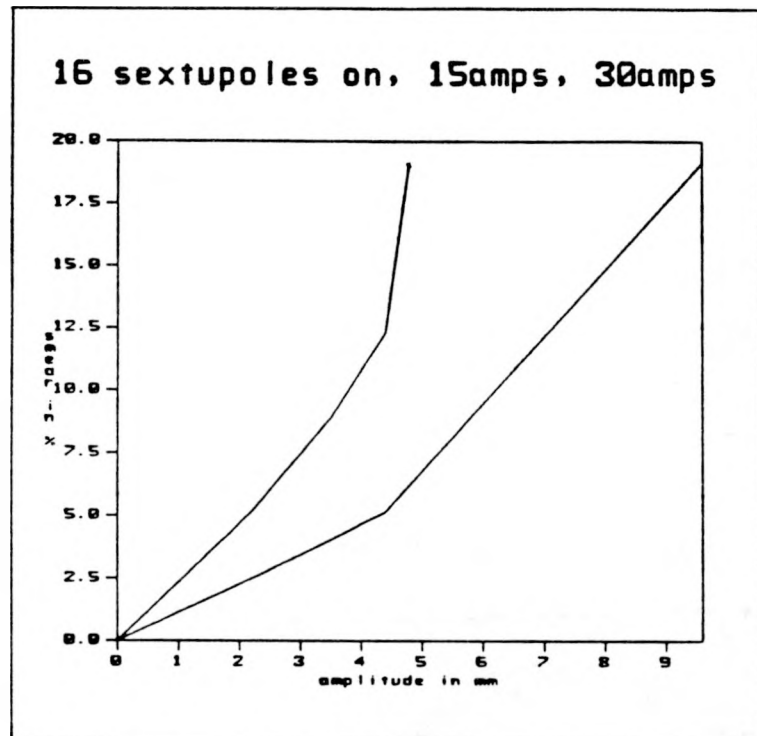
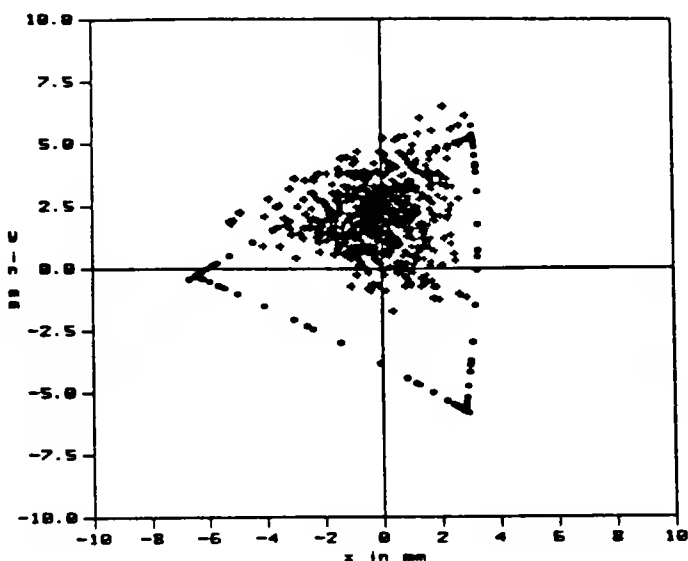


Fig. 6. Calculation of smear versus kick amplitude for a single particle in presence of sextupole distribution used in this experiment. The fractional part of the tune is 0.42.

30 amperes, tune=19.39, 5kv kick



30 amperes, tune=19.39, 10kv kick

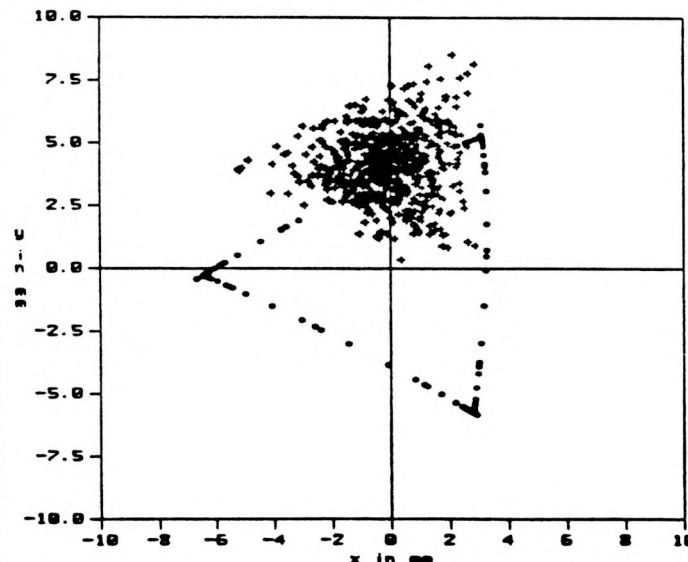
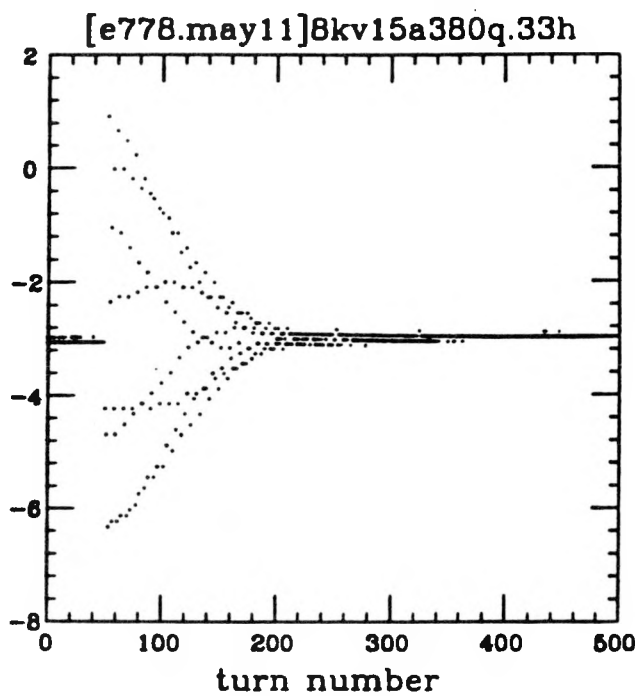
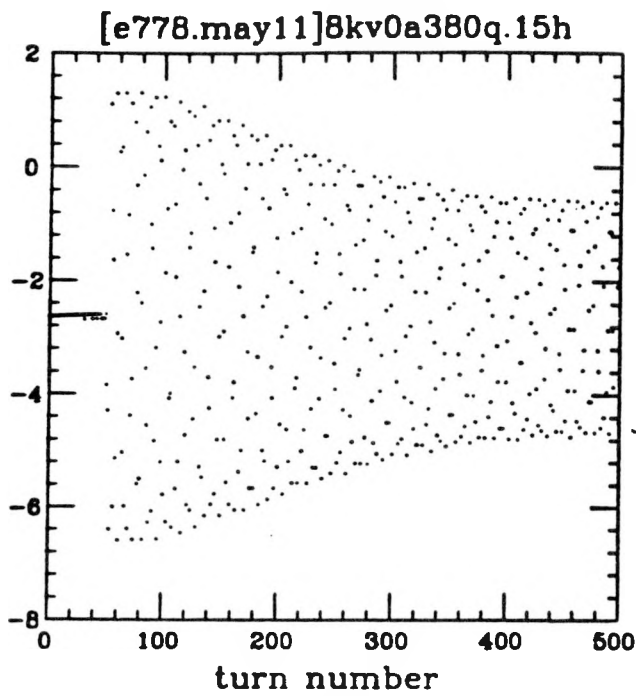


Fig. 7. Simulation of two experimental conditions in phase space at kicker location immediately after beam deflection. The solid curve represents the limit of stability. The dots represent the particle distribution.

first horizontal BPM, x1(mm)



first horizontal BPM, x1(mm)

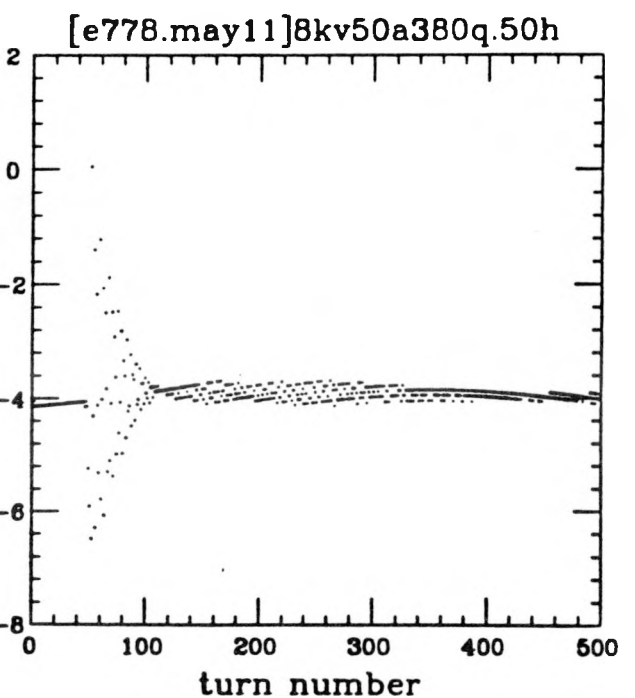
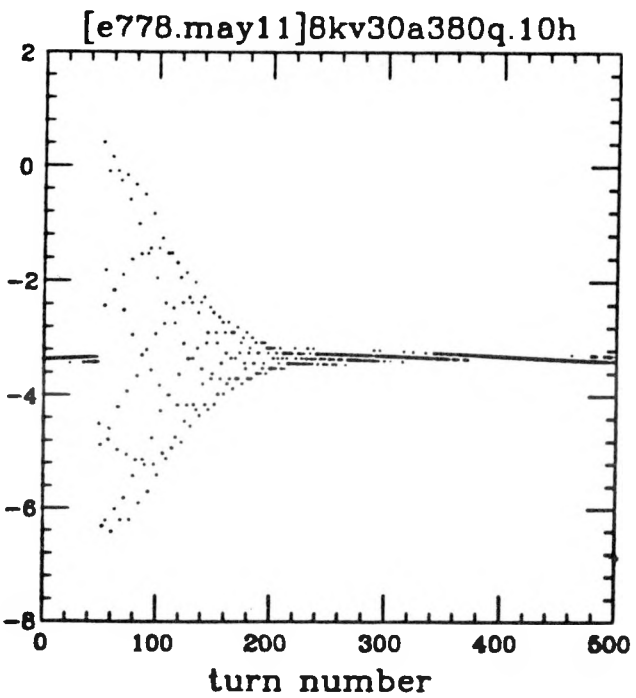


Fig. 8. Experimental turn-by-turn position data illustrating the loss of coherent beam centroid motion for (a) 0 ampere sextupole excitation, (b) 15 amperes, (c) 30 amperes, and (d) 50 amperes.

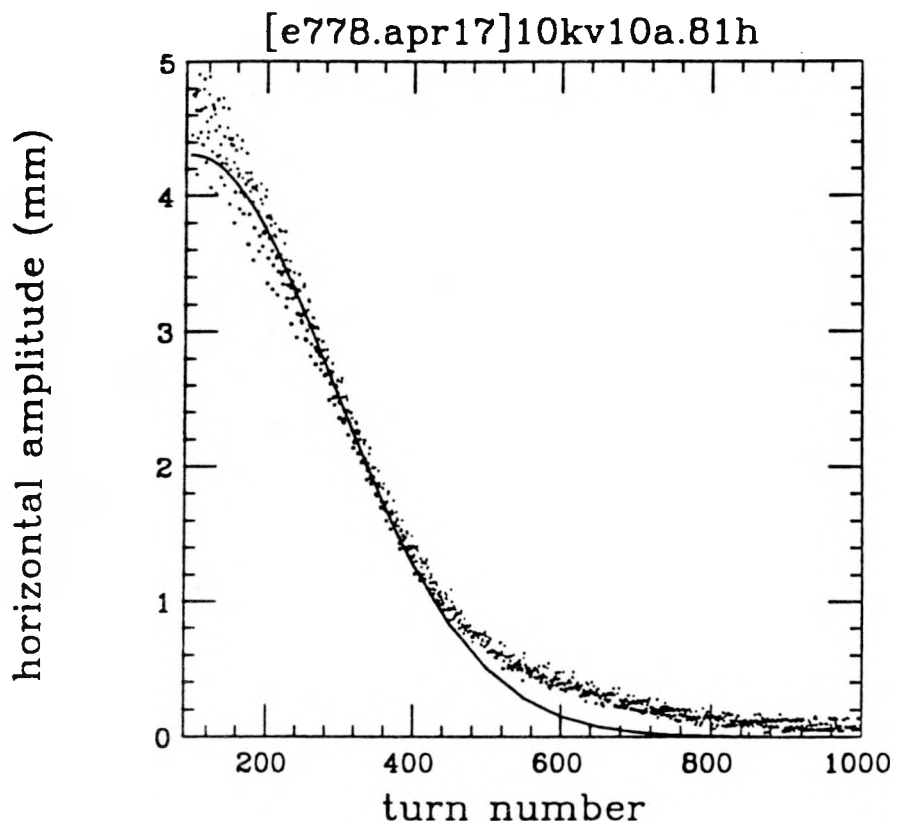


Fig. 9. Reduction of amplitude of the coherent betatron oscillation with turn number for an initial 4 mm kick with sextupoles excited to 10 amperes. The solid line is a fit of the experimental data to a Gaussian.

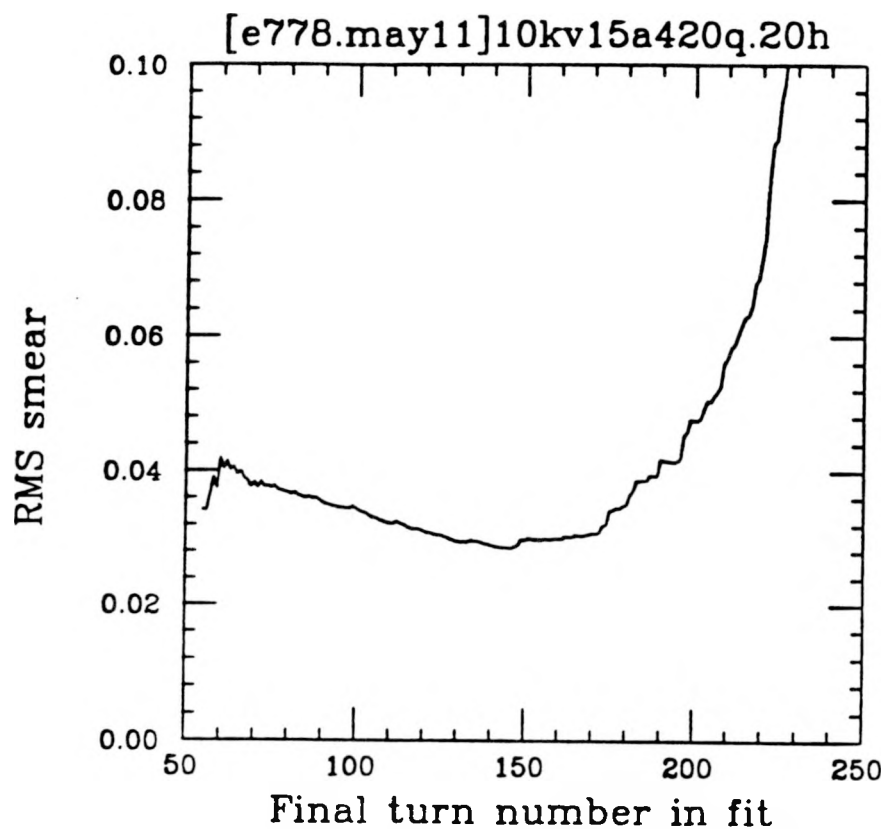


Fig. 10. Smear versus the number of data points used in its computation for a typical experimental condition. The deterioration of the smear determination at large turn numbers is a consequence of the decoherence.

8kv0a380q.15h

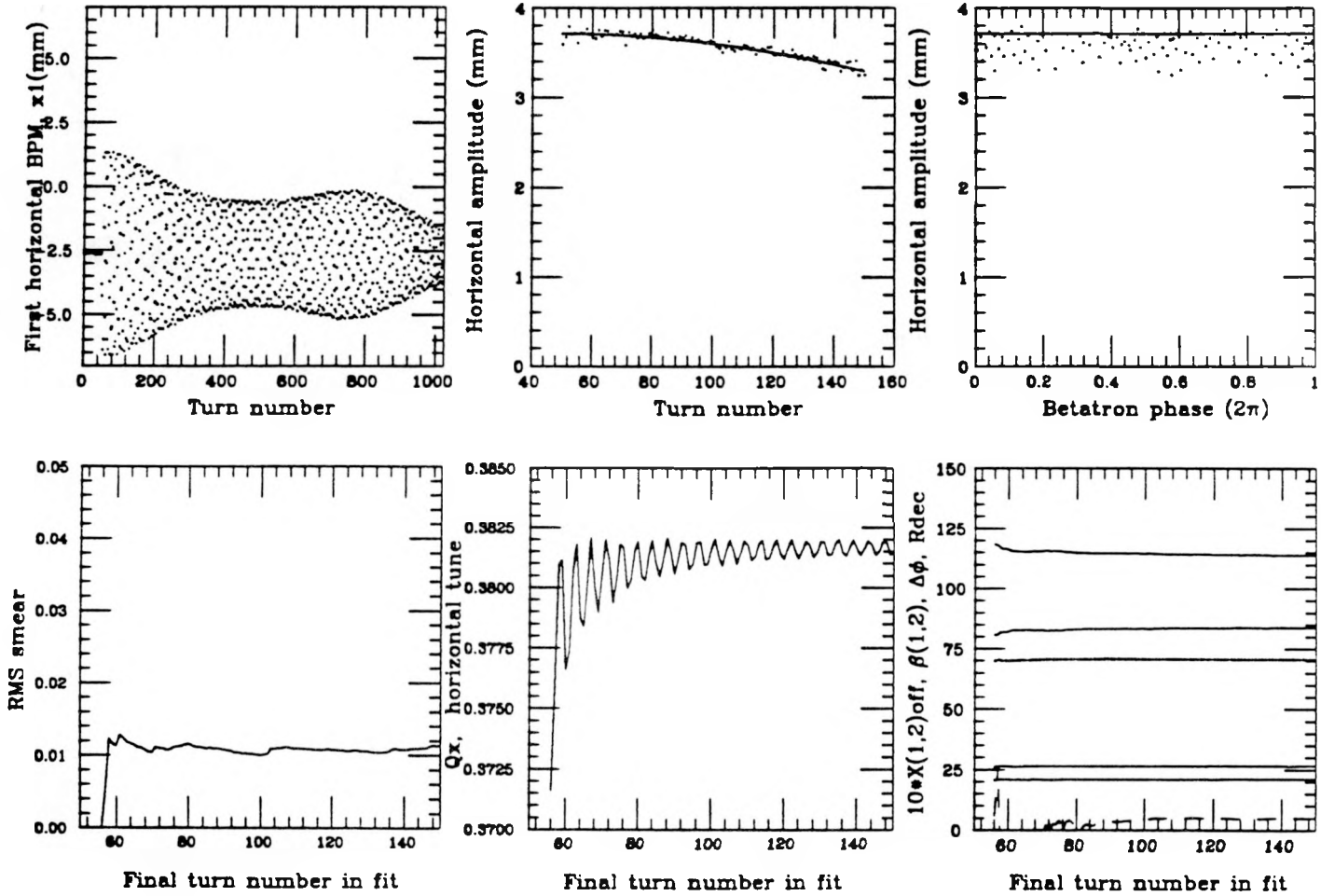


Fig. 11. Output of the program Tevex for a measurement on the bare Tevatron at a tune of 19.38. Clockwise from the upper left hand corner, the plots have the following significance. The first simply reconstructs the raw turn-by-turn data for one of the position monitors used. The next illustrates the amplitude versus turn number and the fit to it. The third shows the amplitude versus oscillation phase; the solid line is the initial amplitude from the fit. The next displays the fitting parameters produced by the least squares calculation. The determination of the tune from the data is reflected in the fifth plot. Finally, the smear is presented in the same fashion as in Figure 10. Note that the smear for the bare Tevatron is at the 1% level.

5kv15a390q.29h

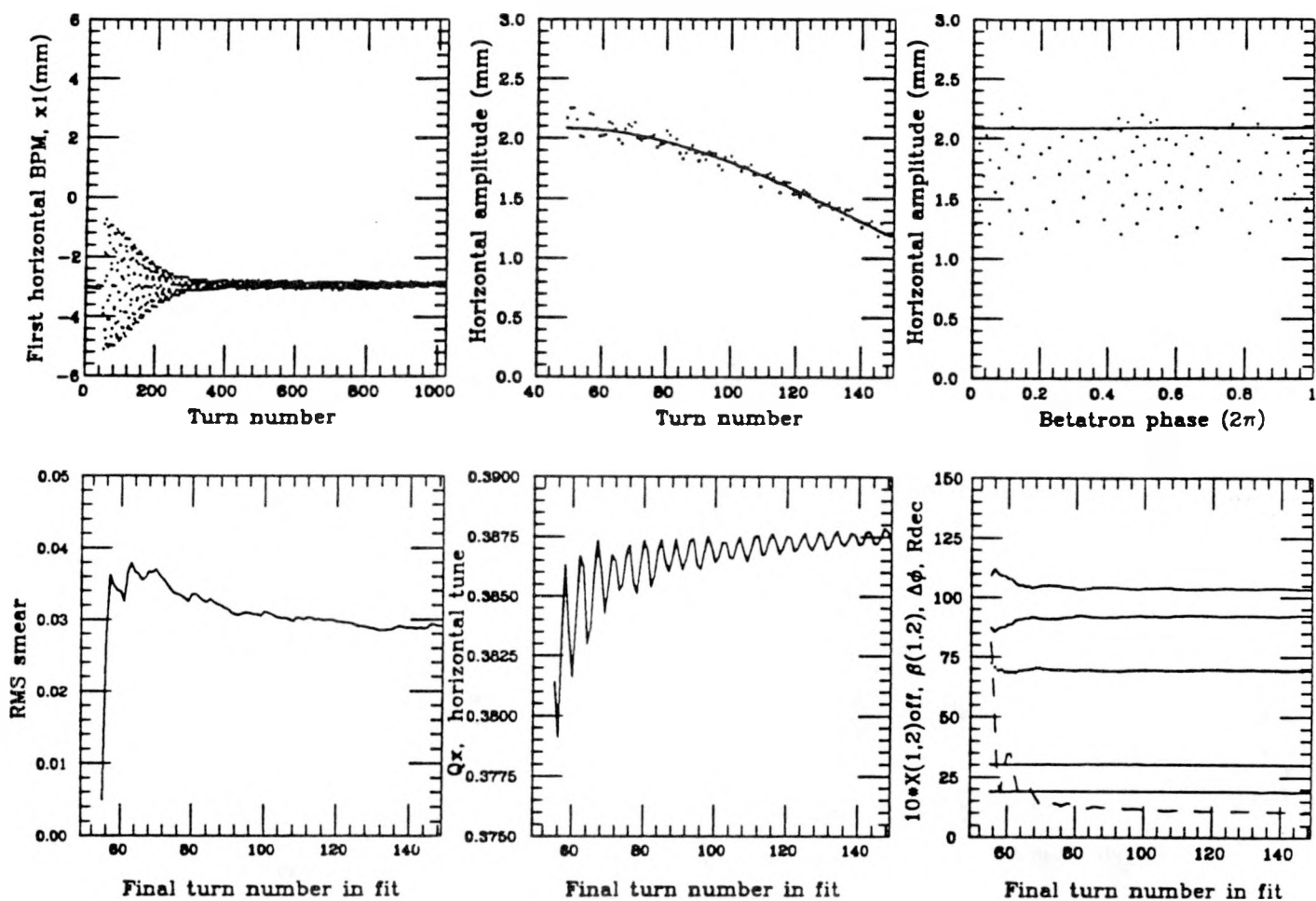


Fig. 12. Output of the program Tevex for a measurement of a kicked beam (kicker voltage of 5 kV) with sextupole excitation of 15 amperes at a machine tune of 19.39.

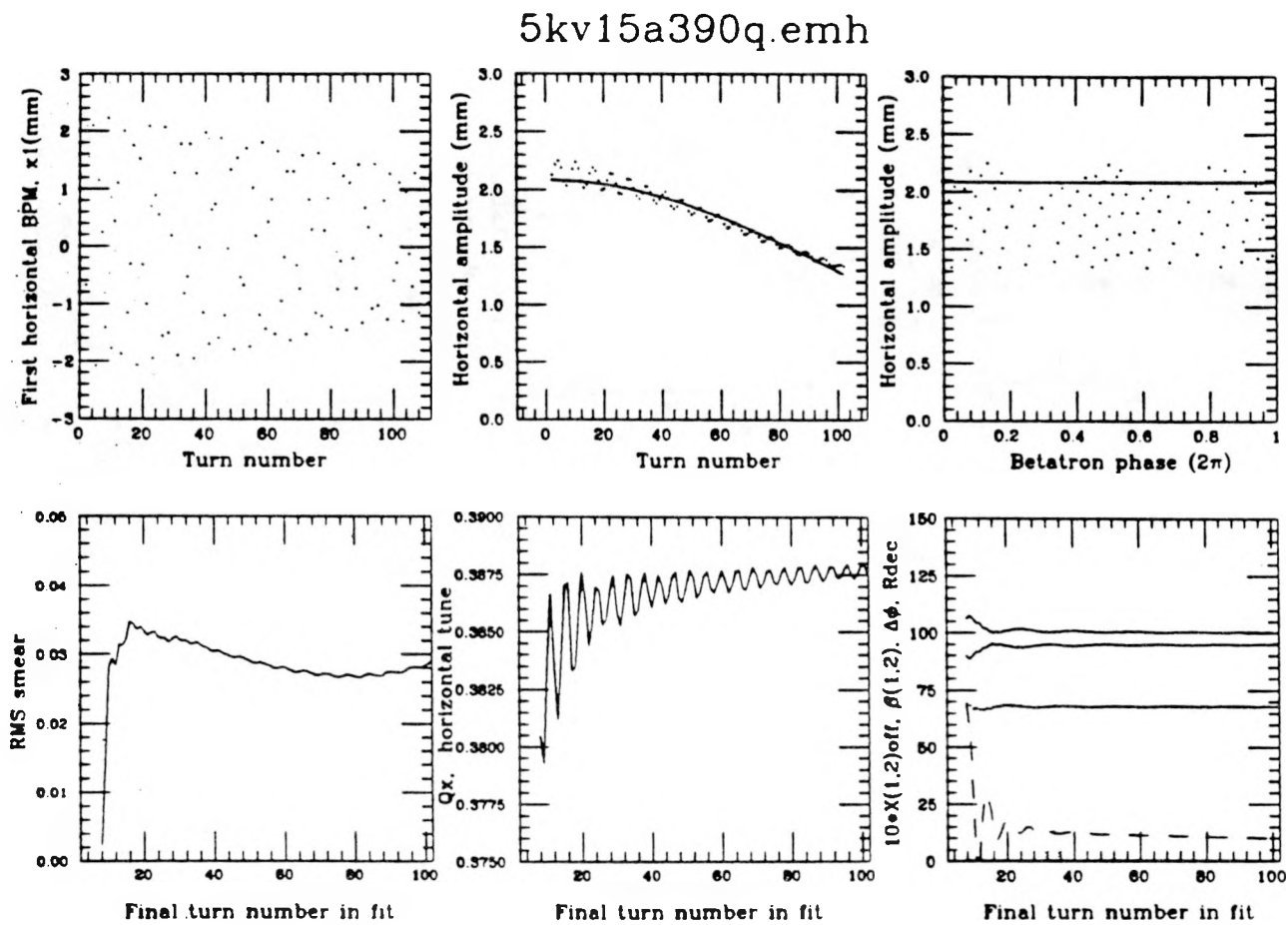


Fig. 13. Output of the program Tevex using simulated data of the same conditions as in Fig. 12. The data was generated using the program Evol, tracking a beam of 600 particles.

5kv15a390q.tmh

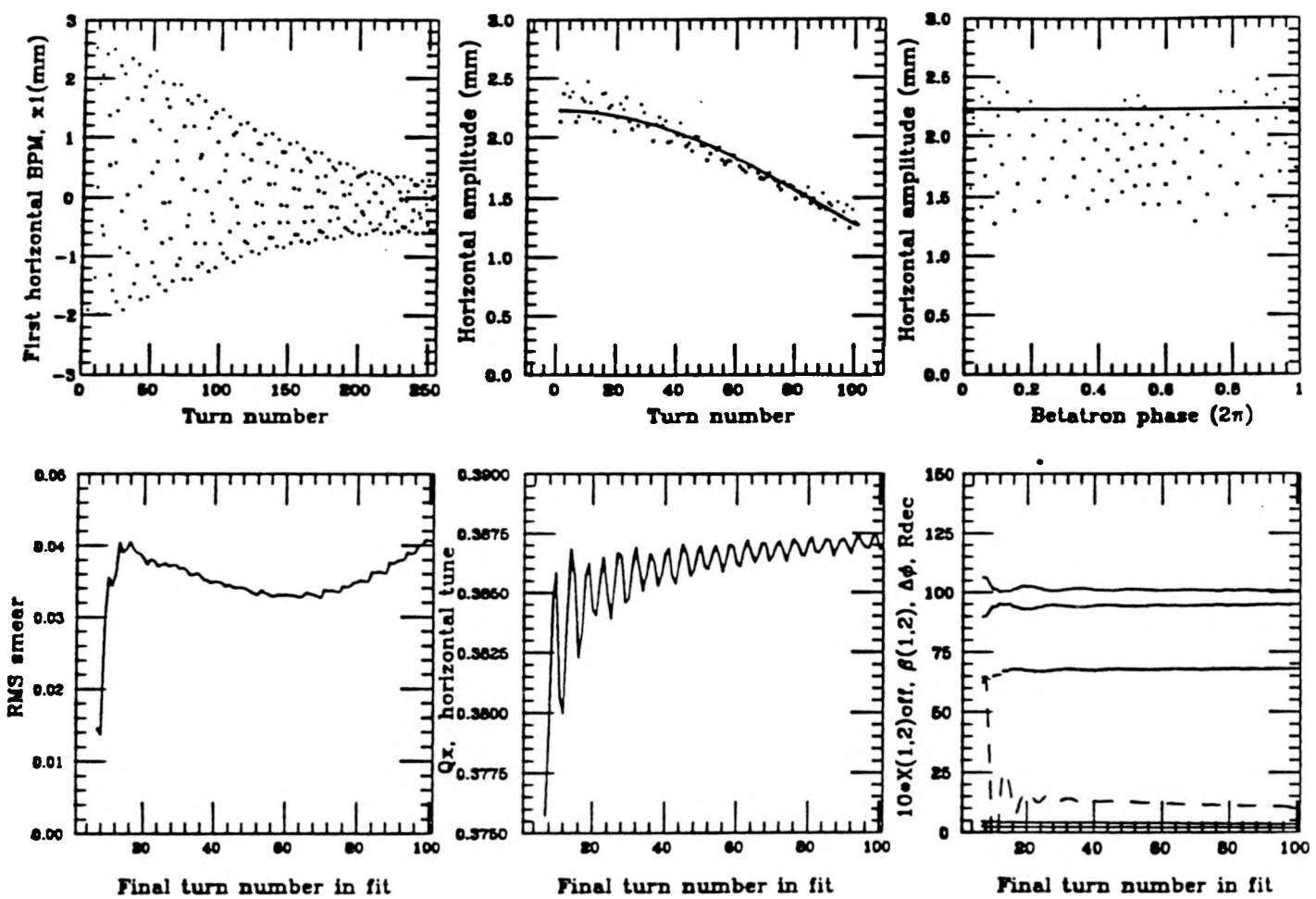


Fig. 14. Output of the program Tevex using simulated data of the same conditions as in Fig. 12. This data was generated using the program Teapot, tracking a beam of 512 particles.

5kv15a390q.amh

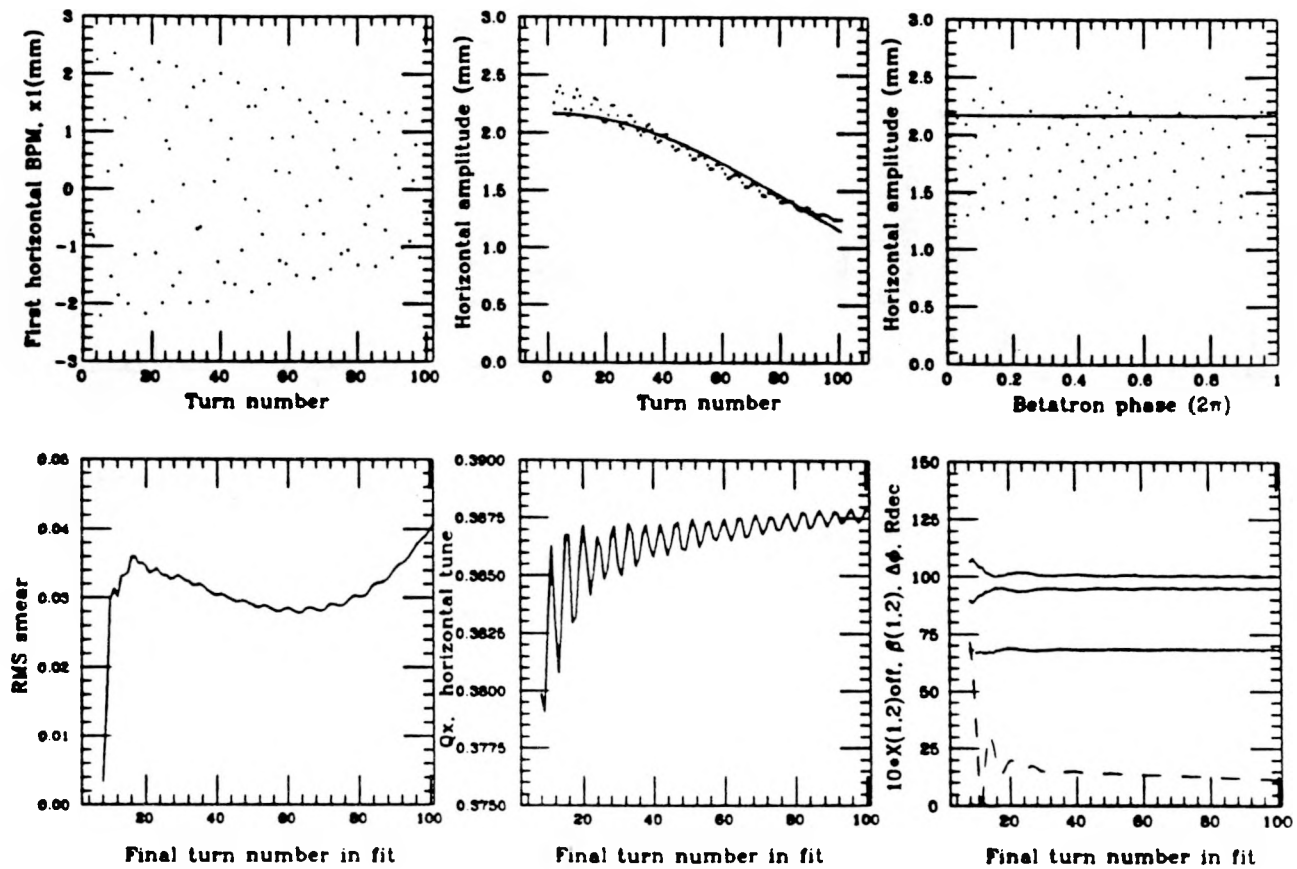


Fig. 15. Output of the program Tevex using simulated data of the same conditions as in Fig. 12. This data was generated using the program Art, tracking a beam of 600 particles.

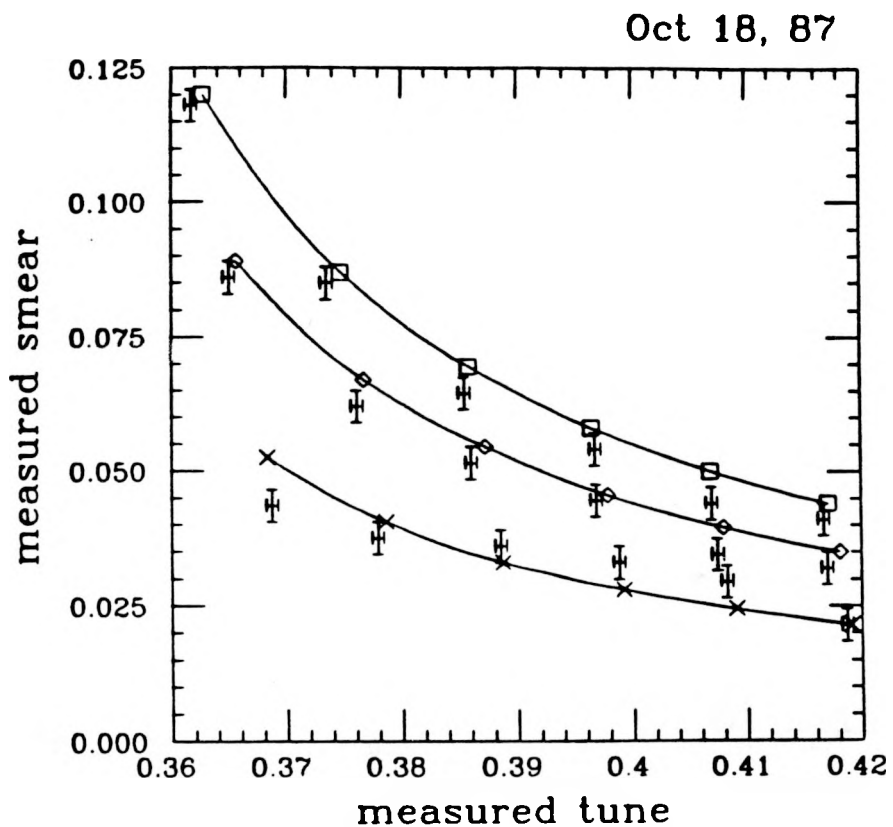


Fig. 16. Summary of smear measurements performed at 15 amperes sextupole excitation and at machine tunes ranging from 19.36 to 19.42. The three solid lines correspond to the results of single particle Evol simulations assuming 5 kV (lower), 7.5 kV (middle), and 10 kV (upper) kicker voltages.

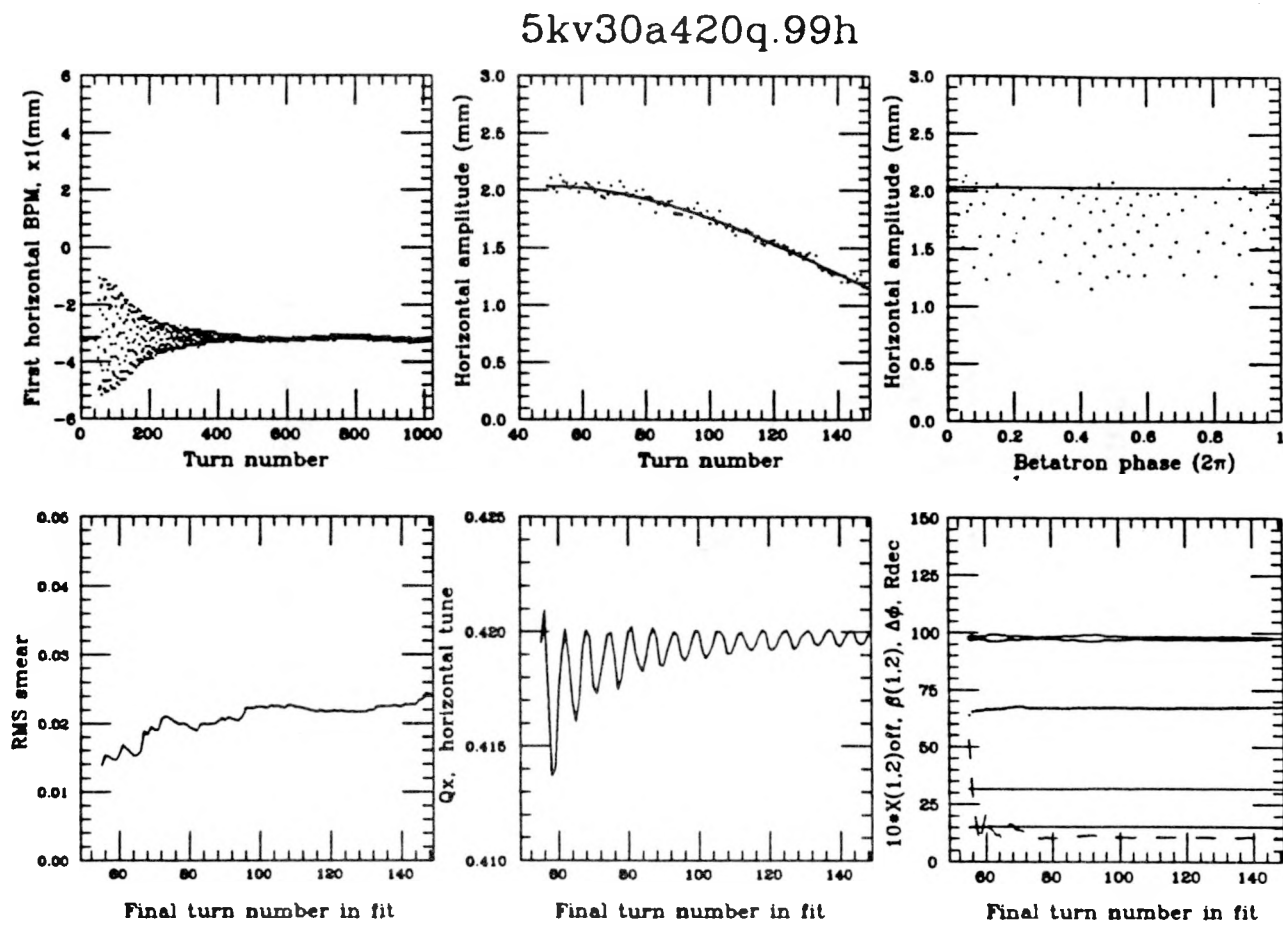


Fig. 17. Output of the program Tevex for a measurement of a kicked beam (kicker voltage of 5 kV) with sextupole excitation of 30 amperes at a machine tune of 19.42.

5kv30a420q.dat

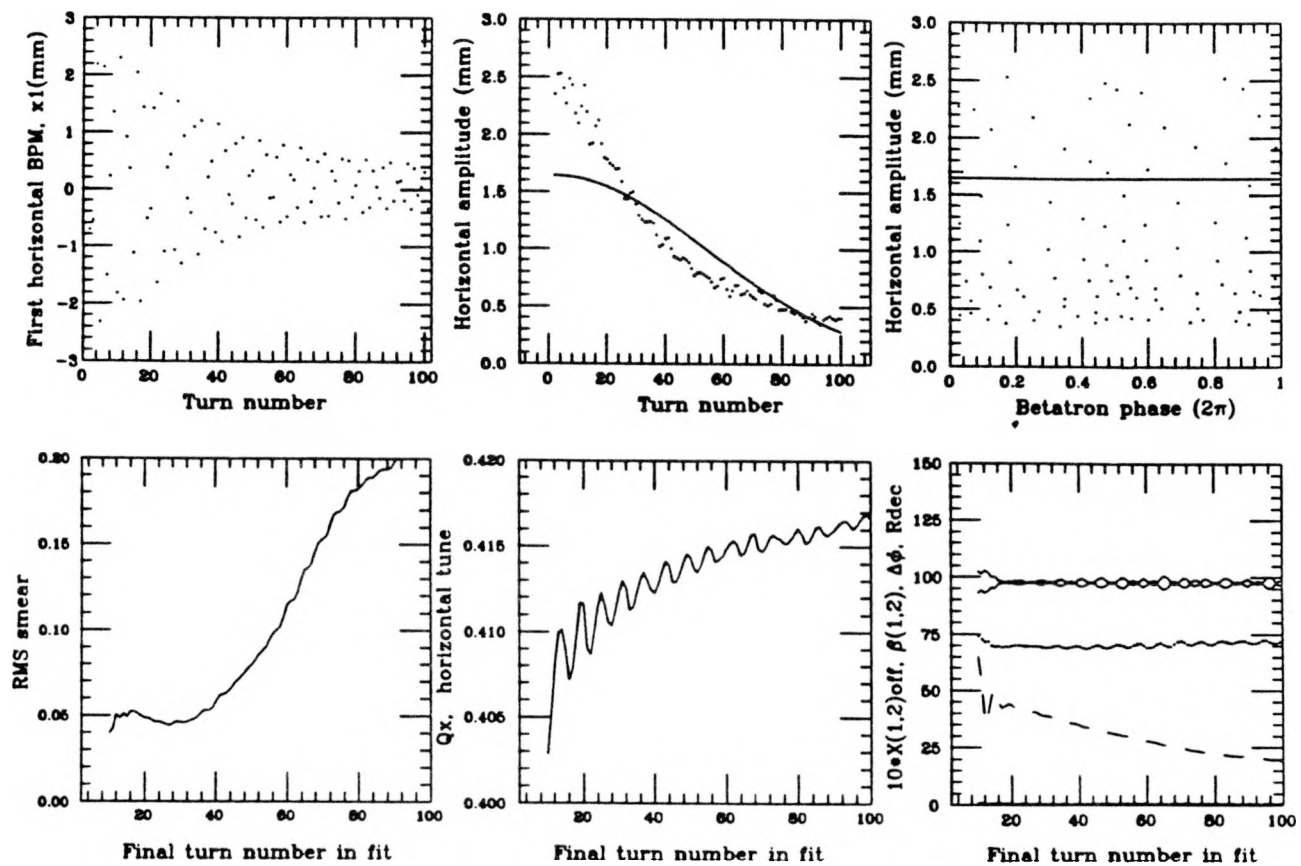


Fig. 18. Output of the program Tevex using simulated data of the same conditions as in Fig. 17. As in the previous figures showing the results of multiparticle tracking, the emittance used in the simulation is the same as that of the actual beam. The data was generated using the program Art, tracking a beam of 600 particles.

5kv30a420q.dat

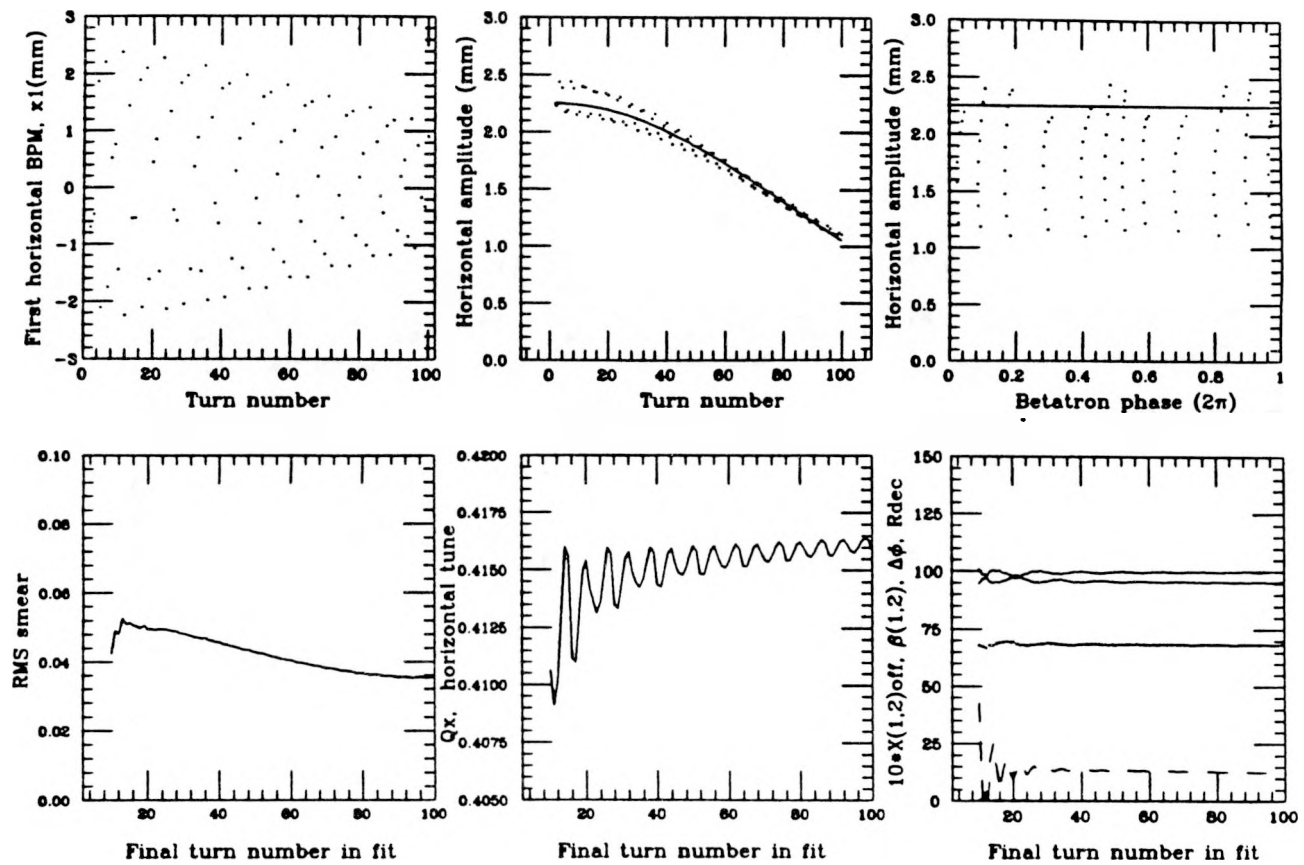


Fig. 19. Output of the program Tevex using simulated data of the same conditions as in Fig. 17, but with the emittance reduced by a factor of four from that actually obtaining in the measurements. This data was generated using the program Art, tracking a beam of 600 particles.

Injection Aperture Measurements

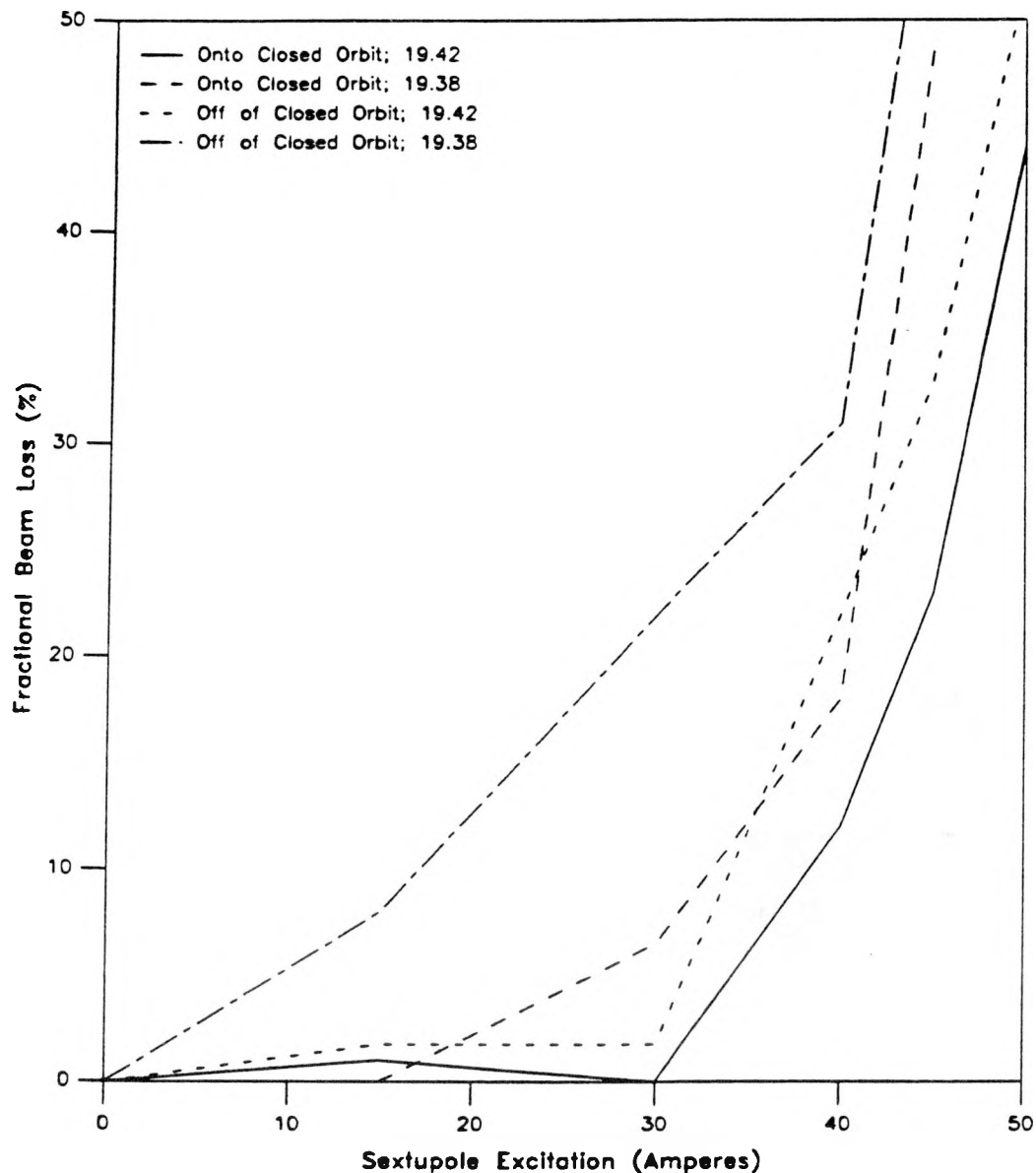


Fig. 20. Fraction of beam lost between injection into the Tevatron and five seconds thereafter versus sextupole excitation. Curves representing injection onto the closed orbit and injection 1.5 mm off of the closed orbit at two different values of machine tune are indicated.

Beam Intensity vs. Time for 45 Amps, tune = 19.42

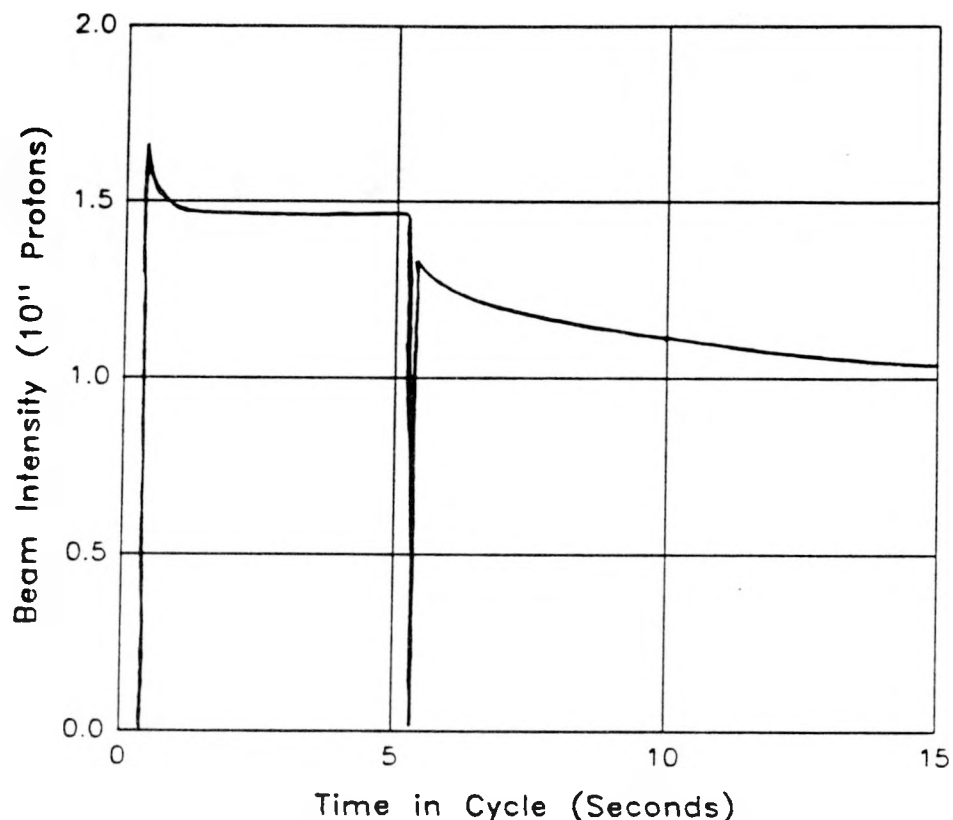


Fig. 21. Beam intensity in the Main Ring and Tevatron as a function of time for a sextupole excitation of 45 amperes and a machine tune of 19.42. The transfer of the beam from the Main Ring to the Tevatron takes place at 5.1 sec. In addition to the initial fast loss of particles upon injection, a slow loss is also evident over the next 10 sec.

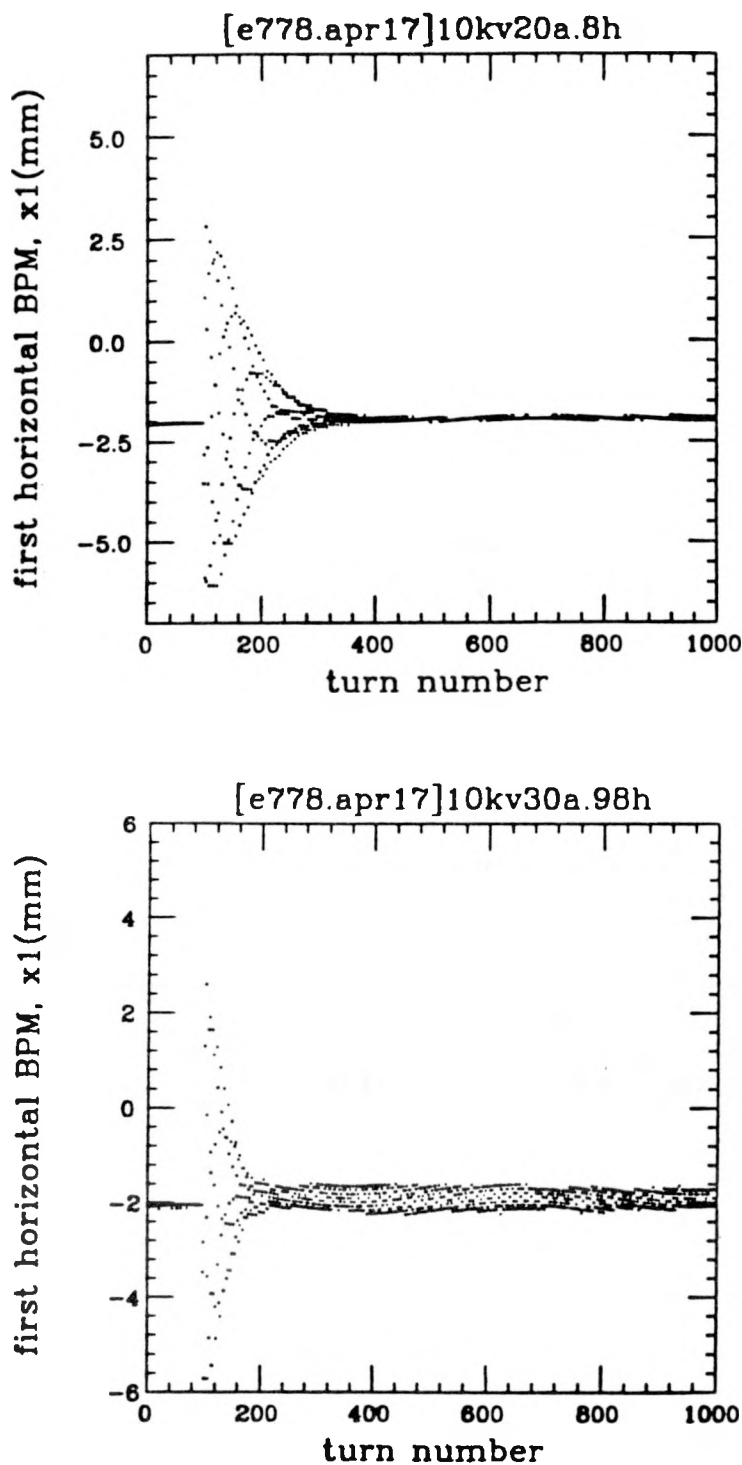


Fig. 22. Illustration of the appearance of a persistent signal in the turn-by-turn data. The upper plot is an example of a typical decoherence of the particle motion. But, the lower plot exhibits a residual signal over the remaining turns.

May 15 modulation measurements

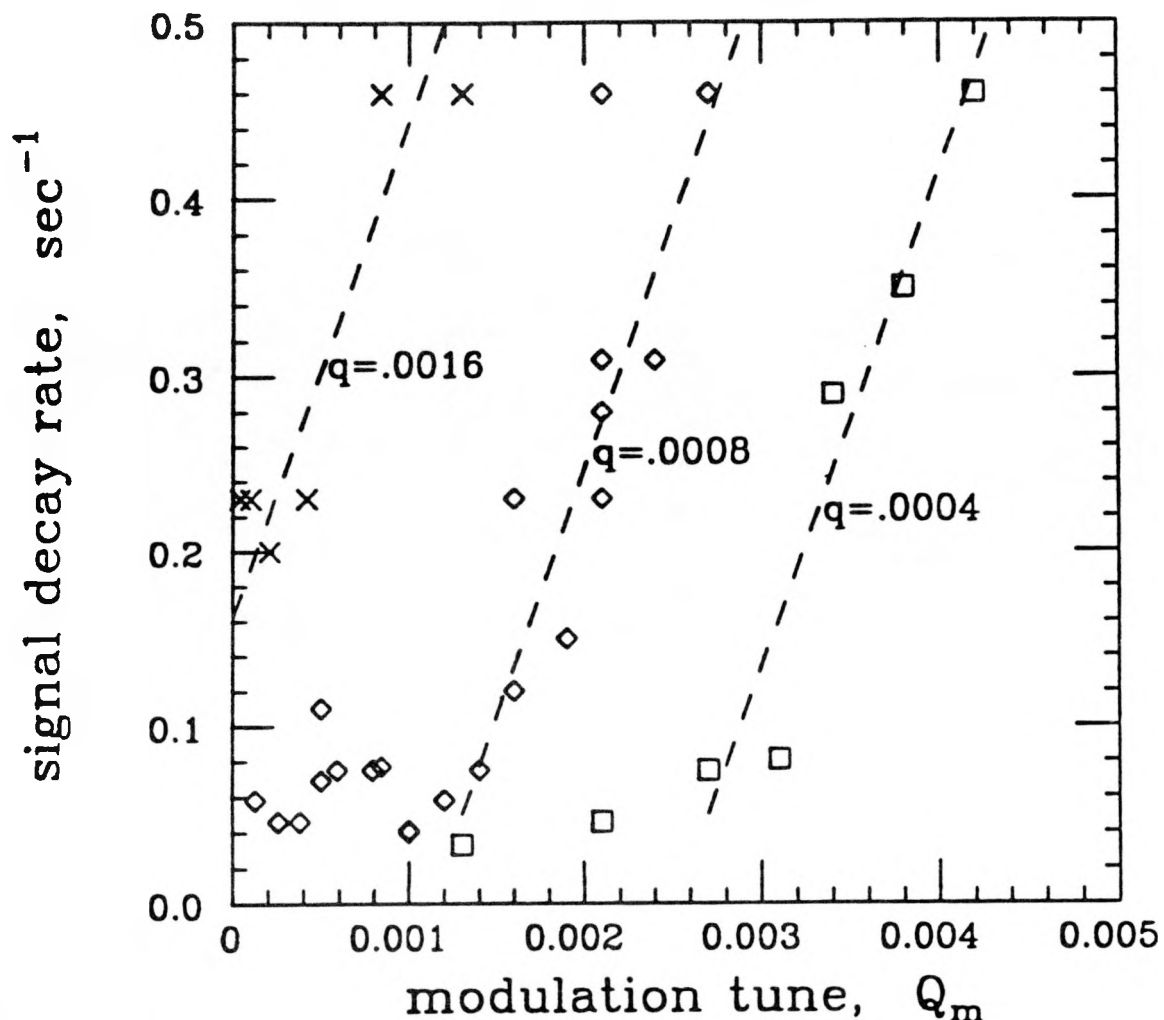


Fig. 23. Rate of decay of persistent tune signal versus the ratio of the tune modulation frequency to the orbit frequency. The three curves represent various values, q , of tune modulation amplitude.

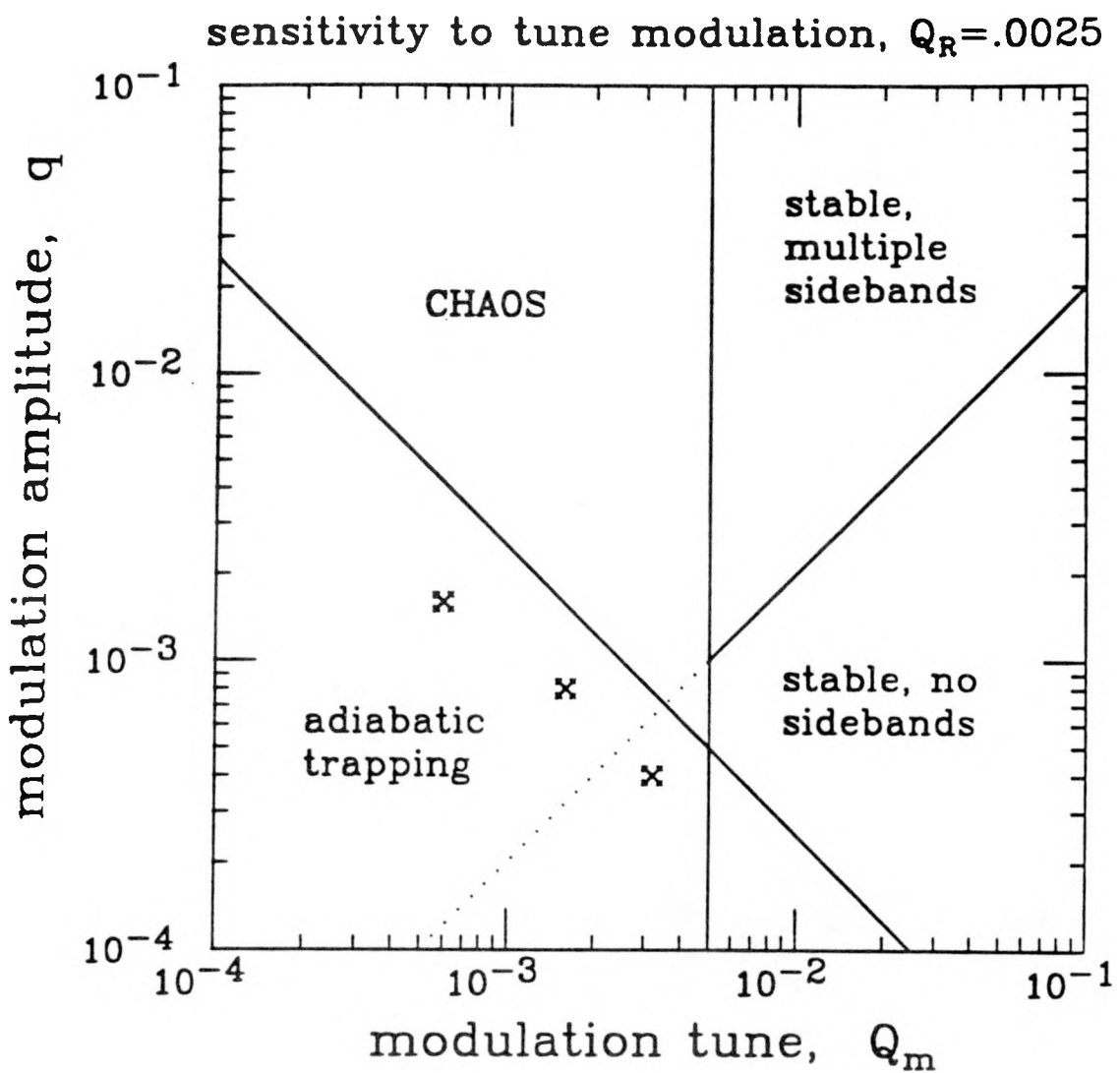


Fig. 24. Plot outlining schematically the regions of stability associated with tune modulation. The three points depict the experimental conditions, but the boundaries were not determined by the experiment. The regions shown here are for a rotation period of 400 turns near the island center ($Q_R = 0.0025$).